Romanian Reports in Physics, Vol. 68, No. 3, P. 1069–1075, 2016

NANOSTRUCTURED Mo-B-C COATINGS

J. BURŠÍK[1], V. BURŠÍKOVÁ[2], P. SOUČEK[2], L. ZÁBRANSKÝ[2], P. VAŠINA[2]

[1]Academy of Sciences of the Czech Republic, Institute of Physics of Materials, Žižkova 22, CZ-61662 Brno, Czech Republic, E-mail: bursik@ipm.cz
[2]Masaryk University, Department of Physical Electronics, Faculty of Science, Kotlářská 2, CZ-61137 Brno, Czech Republic,
E-mails: vilmab@physics.muni.cz; soucek@physics.muni.cz; zerafel@mail.muni.cz; vasina@physics.muni.cz

Received August 31, 2015

Abstract. Microstructure and mechanical properties of thin Mo-B-C layers prepared by magnetron sputtering were studied by means of scanning and transmission electron microscopy and nanoindentation techniques. Depending on sputtering conditions the microstructure changes from amorphous to partly crystalline. No cracks were observed at the substrate-layer interface under indentation prints. The materials showed a promising combination of high hardness and elastic modulus together with high fracture toughness.

Key words: magnetron sputtering, Mo-B-C coating, microstructure, electron microscopy, focused ion beam, nanoindentation.

1. INTRODUCTION

Nanostructuring is a recognized way of preparing novel materials with properties significantly different from their bulk constituents [1]. Nanocomposite thin films, multilayers and nanolaminates were proven in many cases to be superior to conventional protective coatings due to their increased hardness and wear resistance [2–8]. The composite architecture is a step towards independent control of toughness and hardness, which is crucial for many industrial applications, *e.g.* for cutting tools protection [3]. Here hardness must be accompanied with high toughness, which is a property of equal importance as hardness. Surface coatings exhibiting high toughness have high resistance to the formation of cracks under stress and high energy absorbance to suppress crack propagation, thus preventing chipping, flaking, or catastrophic failure. Nowadays the attention is oriented to nanolaminate coatings with thin film structures of high interfacial density [1]. Nanolaminates exhibiting regions of alternating high and low electron densities within the unit cell has been reported [9] for unusual combination of high hardness with moderate ductility and high fracture toughness.

The group of nanolaminate materials includes X_2BC boron and carbon based nanolaminates exhibiting a unique combination of high stiffness and moderate ductility, when X = Ta, Mo or W [9, 10]. However their synthesis temperature above 800 °C impedes effortless applicability as a coating system. This temperature can be substantially reduced by a suitable choice of preparation method [10]. In this paper we report on microstructure and mechanical properties of Mo-B-C layers prepared by magnetron sputtering.

2. EXPERIMENTAL

Samples of 1–2 μm thin layers were prepared using magnetron sputtering of either a Mo_2BC target (samples L1, L2) or a combination of three targets: B_4C, C and Mo (samples L3 and L4). The three targets were used to control the resulting stoichiometry of the deposited layer better. The layers were deposited on either steel or hard metal substrates which were ultrasonically cleaned in a degreasing agent and then placed in the chamber using load-lock system. Furthermore, prior to the deposition process all substrates were cleaned in argon plasma for 20 minutes. The RF bias of −200 V was applied to the substrate holder. The pressure was 0.3 Pa. The deposition conditions are summarized in Table 1.

Table 1

Deposition conditions used to prepare samples L1 to L4, when *p* denotes pulsed power with frequency 350 kHz and duty cycle 65%. Otherwise, the dc power was used

Sample	Power on a target [W]				Bias voltage [V]	Deposition time [min]	Substrate
	B_4C	C	Mo	Mo_2BC			
L1	–	–	–	250 (p)	0	180	hard metal
L2	–	–	–	250 (p)	−200	420	hard metal
L3	104	281	84	–	−200	300	steel
L4	128	250 (p)	110	–	−200	480	hard metal

Microstructure of layers was studied using a Tescan LYRA 3XMU FEG/SEM×FIB scanning electron microscope (SEM), a Philips CM12 STEM transmission electron microscope (TEM) and a JEOL JEM-2100F high resolution TEM. Thin lamellar cross sections for TEM observations were prepared using a focussed ion beam (FIB) in SEM from two locations in each sample: an undisturbed layer and a central region of indentation print made with Berkovich tip with a load of 1 N.

The microstructure observations were correlated with mechanical properties characterized by means of nanoindentation experiments using a Hysitron dual head TI950 triboindenter equipped with a diamond Berkovich tip in both static and

dynamic loading regime in the load range from 50 μN to 11 mN. The hardness and reduced elastic modulus values were determined at indentation depths where the substrate influence was negligible. The fracture toughness of the coatings was evaluated using the nanoindenter equipped with a sharp CubeCorner indenter. Moreover, microindentation using a Fischerscope nanoindenter equipped with Berkovich indenter was used to study the fracture resistance of the coatings in the load range from 0.01 to 1 N. The modulus mapping mode was applied to obtain quantitative maps of the storage and loss stiffness and the storage and loss modulus at nanometer contact depths. During the in-situ scanning the sample's dynamic response to the oscillating load was continuously monitored as a function of the position.

The film composition was studied using combined RBS/ERDA measurements. The film crystallinity was studied using a Rigaku X-Ray Diffractometer SmartLab Type F.

3. RESULTS AND DISCUSSION

SEM observations of the Mo-B-C layers reveal smooth surface and uniform structure on cross sections. TEM imaging of thin lamellas and selected area electron diffraction (SAD) were used to study microstructure in detail. Fig. 1a shows the cross section of layer L1 with hard metal substrate below and Pt protective layer above. SAD pattern in Fig. 1a inset indicates diffuse rings typical of amorphous material. TEM micrograph in Fig. 1b shows layer L3 with about 100 nm thick Mo interlayer below and a steel substrate at the bottom. Nanosized objects are observed in the amorphous Mo-B-C matrix. The SAD pattern in the inset shows diffuse rings similar to those in Fig. 1a, however, the uneven intensity distribution reflects partly crystalline structure of layer L3. Figure 2 shows details of microstructure observed in TEM at high resolution: the amorphous structure of layer L1 close to WC grain of substrate (Fig. 2a) and a crystalline nanoparticle surrounded by amorphous volume in layer L3 (Fig. 2b).

To test the quality of the layers and their protective power, the deformed regions under indentation prints were studied. A relatively high indentation load of 1 N was used, which produced indents of the size of about 10 μm, *i.e.* the indentation depth of about 1.5 μm. Even under such severe conditions we did not observe any interfacial cracks or other defects in any of the studied samples. Figure 3 shows deformed microstructure of layer L1. The substrate under the indenter is dished and the interface is wavy. Detail in Fig. 3b shows heavily deformed grains of hard metal substrate, while at the same time the interface and layer stay free of defects.

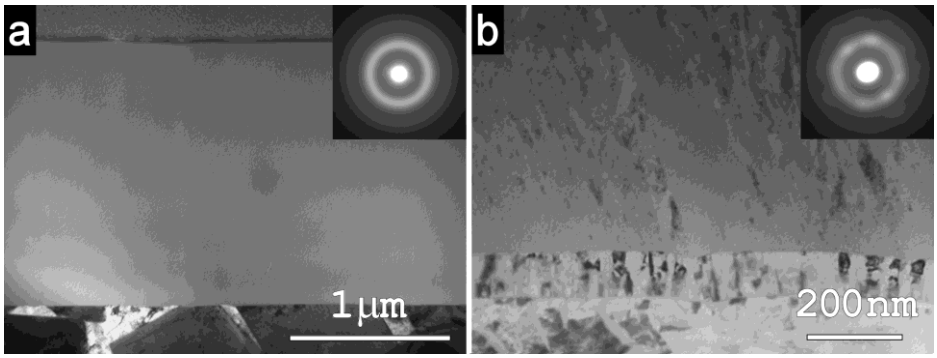

Fig. 1 – TEM micrographs and SAD patterns of thin lamellas of sample L1 ((a), amorphous Mo-B-C layer on hard metal substrate) and L3 ((b), partly crystalline nanostructured Mo-B-C layer on Mo interlayer and steel substrate).

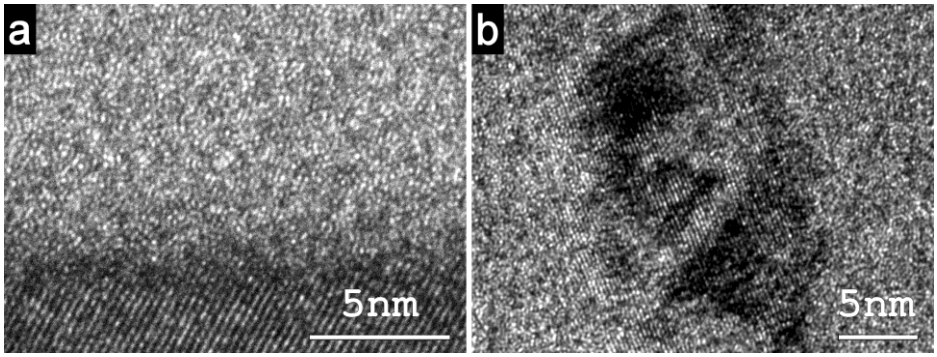

Fig. 2 – HRTEM micrographs of sample L1 ((a), amorphous Mo-B-C layer on WC grain of hard metal substrate) and L3 ((b), crystalline region embedded in amorphous Mo-B-C).

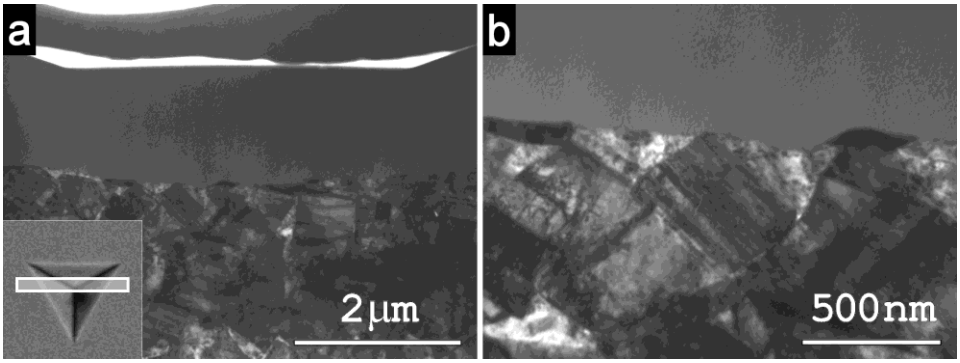

Fig. 3 – TEM micrographs of lamellas under indentation prints. Layer L1 on hard metal, inset with SEM image of indentation print shows schematically the region selected for lamella preparation by FIB (a). A detail of layer/substrate interface (b).

Mechanical properties were studied in a broad load range from 50 μN to 1 N. In Table 2 the mechanical properties of the coatings prepared according to deposition parameters listed in Table 1 are compared to the material parameters of Mo_2BC coatings reported in [9] and to the elastic modulus, which was calculated for single-crystalline Mo_2BC using *ab-initio* method. The coating reported in [9] was prepared using dc magnetron sputtering from three plasma sources at a substrate temperature of about 900 ^oC.

Table 2

Mechanical properties and structure of samples L1 to L4 compared to the values presented in [9]

Sample	Hardness [GPa]	E_r [GPa]	H/E_r	H^3/E_r^2 [GPa]	Structure
Theoretical [9]	–	470	–	–	Crystalline
Measured [9]	29 ± 2	460 ± 21	0.063	0.115	Nanocrystalline
L1	19.0 ± 0.5	267 ± 5	0.071	0.096	Amorphous
L2	19.5 ± 0.5	276 ± 5	0.071	0.097	Amorphous
L3	28.5 ± 0.7	310 ± 4	0.092	0.240	Nanocomposite
L4	31.6 ± 0.8	345 ± 9	0.092	0.265	Nanocomposite

The hardness values of amorphous Mo-B-C coatings L1 and L2 prepared using Mo_2BC target at pulsed power with frequency of 350 kHz and duty cycle of 65% are comparable with common hard amorphous hydrogenated diamond-like carbon (a-C:H) coatings [11, 12]. However, their elastic modulus and fracture toughness is significantly higher. In case of the use of Mo_2BC target the prepared coatings atomic composition was far from the stoichometric composition according to RBS/ERDA studies. Therefore their structure was completely amorphous. The use of three targets, B_4C, C and Mo, turned out to be more successful to approach the Mo_2BC stoichometric composition. According to XRD and TEM observations the samples were partially crystallised and showed nanocomposite structure. Although the coatings L3 and L4 were prepared without substrate heating, their hardness values are comparable with the values achieved in [9]. Due to the amorphous matrix, the elastic modulus of prepared coatings is slightly lower. However the H/E_r and H^3/E_r^2 ratios, which are measures of the toughness and resilience of the coating, are higher for all samples L1 to L4. These parameters play an important role in industrial applications of protective coatings. Toughness can be defined as the ability of a material to absorb energy during deformation up to rupture [13–15]. For comparison the highest H/E values achievable are about 0.04 with heat-treated tool steel, about 0.06 for ceramics like Al_2O_3, ZrO_2, Si_3N_4 or SiC and about 0.08 for nitride based coatings like TiN and CrN [16]. The H/E values of amorphous coatings L1 and L2 are comparable with the above listed values, the nanocomposite samples L3 and L4 exhibit even higher H/E values. The prediction

of the wear of the coatings can be based on the resilience of the coating, which is defined as the resistance of a material against plastic deformation and relates to the ratio of H^3/E_r^2 [15]. According to Tab. 2, the highest H^3/E_r^2 were obtained in the case of nanocomposite samples L3 and L4.

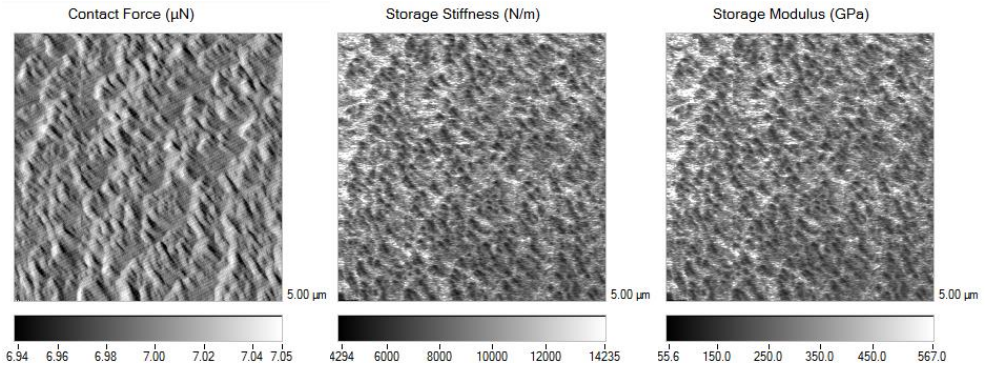

Fig. 4 – Example of modulus mapping results on sample L4 on a hard metal substrate. The maps of the contact force (on the left), storage stiffness (in the middle) and storage modulus (right) were obtained with oscillation amplitude of 2.8 μN and oscillation frequency of 300 Hz on area of 5×5 μm^2.

The modulus mapping capability was applied to obtain quantitative maps of the storage and loss stiffness and the storage and loss modulus. The modulus mapping combines the in-situ imaging capabilities with the ability to perform nanodynamic mechanical analysis. In Fig. 4 an example of the modulus mapping results obtained on sample L4 at oscillation frequency of 300 Hz and oscillation amplitude of 2.8 μN is shown. The storage stiffness and storage modulus maps illustrate the nanocomposite behavior of the tested sample. The stiff crystalline areas with elastic moduli achieving the predicted value [9, 10] and the areas with softer amorphous phase are clearly distinguishable.

The excellent fracture resistance of coatings L1 to L4 was proven using two methods. The nanoindentation technique with sharp cube corner diamond indentor was used to test the resistance of coatings against crack creation. There was no crack initiation in the nanoindentation load region (50 μN – 11 mN). Therefore microindentation tests were carried out with Berkovich indenter in the region from 0.01 to 1N. Even at the highest indentation load of 1 N it was not possible to generate cracks either in the coatings or at the coating/substrate interface as it is shown in Figs. 1 and 3.

4. CONCLUSION

Several Mo-B-C thin films with different structures were prepared using magnetron sputtering. The Mo-B-C coatings showed a promising combination of

high hardness and elastic modulus together with high fracture toughness due to predominant plastic behavior. The hardness of amorphous Mo-B-C coatings was found around 19.5 GPa which was comparable with standard DLC coatings and the elastic modulus of about 270 GPa. Using the cube corner indenter with loads up to 10 mN and using Berkovich tip with loads up to 1 N the differential hardness curves and TEM images from the area under the indentation imprint proved that there was no crack formation in the vicinity of the imprint. Also the adhesion after indentation up to 1 N remained sufficient and no delamination occurred.

Acknowledgements. This work was supported by the Czech Science Foundation (Grant Project No. 15-17875S).

REFERENCES

1. J. Azadmanjiri, C.C. Berndt, J. Wang, A. Kapoor, V.K. Srivastava and C. Wen, J. Mater. Chem. **A 2**, 3695 – 3708 (2014).
2. S. Vepřek, J. Vac. Sci. Technol. **A 17**, 2401 – 2419 (1999).
3. J. Musil, Surf. Coat. Technol. **125**, 322 – 330 (2000).
4. P.H. Mayrhofer, Prog. Mater. Sci. **51**, 1032 – 1114 (2006).
5. P. Vašina, P. Souček, T. Schmidtová, M. Eliáš, V. Buršíková, M. Jílek, M. Jílek Jr., J. Schäfer and J. Buršík, Surf. Coat. Technol. **205**, S53 – S56 (2011).
6. A.A. Voevodin, J.S. Zabinski, C. Muratore, Tsinghua Sci. Technol. **10**, 665 – 679 (2005).
7. R. Žemlička, M. Jílek, P. Vogl, P. Souček, V. Buršíková, J. Buršík and P. Vašina, Surf. Coat. Technol. **255**, 118 – 123 (2014).
8. A.D. Pogrebnjak, A.P. Shpak, N.A. Azarenkov and V.M. Beresnev, Physics – Uspekhi **52**, 29 – 54 (2009).
9. J. Emmerlich, D. Music, M. Braun, P. Fayek, F. Munnik and J.M. Schneider, J. Phys. D: Appl. Phys. **42**, 185406 (2009).
10. H. Bolvardi, J. Emmerlich, S. Mráz, M. Arndt, H. Rudigier and J.M. Schneider, Thin Solid Films **542**, 5 – 7 (2013).
11. A. Grill, Diam. Relat. Mater. **8**, 428 – 434 (1999).
12. D. Franta, V. Buršíková, I. Ohlídal, P. Sťahel, M. Ohlídal, D. Nečas, Diam. and Relat. Mater. **16**, 1331 – 1335 (2007).
13. Y.T. Pei, D. Galvan, J.Th.M. De Hosson, A. Cavaleiro, Surf. Coat. Technol. **198**, 44 – 50 (2005).
14. D. Martínez-Martínez, C. López-Cartes, A. Fernández, J.C. Sánchez-López, Thin Solid Films **517**, 1662 – 1671 (2009).
15. P. Souček, T. Schmidtová, L. Zábranský, V. Buršíková, P. Vašina, O. Caha, J. Buršík, V. Peřina, R. Mikšová, Y.T. Pei, J.Th.M. De Hosson, Surf. Coat. Technol. **255**, 8 – 14 (2014).
16. C. Donnet, A. Erdemir, *Tribology of Diamond-like Carbon Films*, Springer, New York, 2008.